Solid-State Adducts between C_{60} and Decamethylferrocene

Aldo Arrais,[a] Eliano Diana,[a] Roberto Gobetto,[a] Marco Milanesio,[b] Davide Viterbo,[b] and Pier Luigi Stanghellini*[b]

Keywords: Donor-acceptor systems / Fullerenes / Infrared spectroscopy / Raman spectroscopy / Sandwich complexes

Co-deposition from concentrated solutions of C_{60} and $Fe[C_5(CH_3)_5]_2$ affords two solid products in different yields. The major product **1**, in the form of regular shaped crystals, has been investigated by X-ray diffraction, ^{13}C CPMAS NMR and vibrational spectroscopy, which showed it to be a cocrystalline adduct of C_{60} and $Fe[C_5(CH_3)_5]_2$ with no significant electron charge transfer between the two building blocks. The minor product **2**, in the form of an amorphous powder, has been investigated by vibrational techniques. Both IR and Raman spectra are consistent with a solid structure in which electron transfer between the two units appears to be possible.

Introduction

Interesting chemical and physical properties indicate fullerene C_{60} to be a useful building block for the preparation of new materials with particular electronic and magnetic properties.[1−4] C_{60} behaves as a mild electron acceptor, capable of incorporating up to six electrons in the cage[5−8] and of forming salts with several inorganic and organic cations.[9] The most fascinating example of these species are the alkali metal salts M_nC_{60}, which show superconductivity properties at quite high temperatures.[10−11]

On the other hand, C_{60} can form molecular adducts with several organic and organometallic electron donors D,[12−22] giving rise to molecular charge-transfer (CT) complexes $D_n(C_{60})$. Presumably, there is no neat distinction between ionic complexes and CT molecular complexes, in that the formally neutral systems probably imply some electron transfer from the donors to C_{60} through π-stacking interactions, particularly favourable when the donor exhibits a largely delocalised π-structure. It might be expected that even a fractional electron transfer should change the spectroscopic (vibrational and magnetic) properties of both the donor and the C_{60} acceptor. Spectroscopic data on C_{60} and its anions are available in the literature, and while they usually indicate that the effect of the charge on the cage is not very evident, careful study can allow their extents to be estimated.[23−27] A clear example is given by the ionic salt $[TDAE]^+[C_{60}]^-$ [TDAE = tetrakis(dimethylamino)ethylene]: the transfer of one electron from TDAE to C_{60} has been associated with subtle modification of the Raman spectrum of C_{60} itself.[28] A parallel opportunity is offered by changes in the spectroscopic properties of the donor molecule as a consequence of electron transfer.[29]

On the basis of our knowledge of the metallocene complexes and their cations, primarily ferrocene (Fc) and decamethylferrocene (*Fc),[30,31] we performed the reaction between C_{60} and *Fc, and the products have been characterised by vibrational and NMR spectroscopy and, when possible, by X-ray diffraction methods. The results, also in comparison with the spectroscopic data concerning the well-known $C_{60}(Fc)_2$,[14] form the object of this paper.

Results and Discussion

Adduct 1

Description of the Structure

The main features of the crystal structure of the adduct **1** are illustrated in Figures 1 and 2. The C_{60} molecule sits with the centre of the "ball" on a crystallographic inversion centre. There are two different types of *Fc molecules: one (molecule A with Fe1 atom) in a general position and one (molecule B with Fe2 atom) with the iron atom sitting on a crystallographic inversion centre. Both rings of molecule A (Figure 1) face two pentagons of the fullerene, in an almost staggered way, and without relevant side shift. On the other hand, molecules B form unconnected layers between the layers of $C_{60}[{*Fc}_2(A)]$ complexes (Figure 2). In these last layers, each fullerene molecule is surrounded by four

---

[a] Dipartimento di Chimica I.F.M., Università di Torino,
via P. Giuria 7, 10125 Torino, Italy
[b] Dipartimento di Scienze e Tecnologie avanzate, Università del Piemonte Orientale "A. Avogadro",
corso T. Borsalino 54, 15100 Alessandria, Italy
Fax: (internat.) + 39-0131/287416
E-mail: pierluigi.stanghellini@mfn.unipmn.it

Supporting information for this article is available on the WWW under http://www.eurjic.org or from the author.

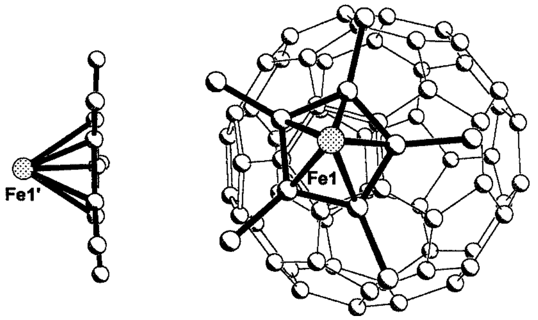

Figure 1. The two different staggered facings of the two *Cp moieties linked to Fe1 and Fe1′ (molecule A) with the five-membered rings of fullerene

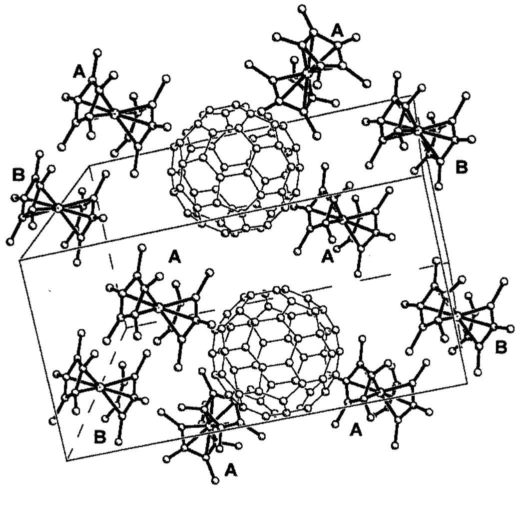

Figure 2. Crystal packing of adduct **1**, showing both the interacting (A) and the non-interacting (B) *Fc molecules in the unit cell

*Fc(A) molecules. The facing of the two rings of molecule A is rather different: one is almost parallel to the pentagon of the C_{60} ring [dihedral angle 4.7(8)°], with a centre-to-centre distance of 3.26(1) Å, while the other is tilted by 14.0(8)°, with a centre-to-centre distance of 3.35(1) Å. The values of the centre-to-centre distances are typical of π interactions between aromatic molecules and are in keeping with the interplane distance of 3.35 Å in graphite. The facing is stabilised by a number of weak C−H···π interactions between methyl hydrogen atoms and fullerene six-membered rings. The shortest distances are found for hydrogen atoms linked to C17 [distance from H to the centre of the ring: 2.94(3) Å] and to C18 [distance from H to the centre of the ring: 2.80(3) Å], belonging to the cyclopentadienyl ring most tilted with respect to the fullerene pentagon. This may suggest that the tilting allows better anchoring of the ring to C_{60}, hindering its free rotation as a sort of a wedge. All other "H-to-ring" distances are greater than 3.0 Å.

The geometry of the fullerene molecule shows the usual bimodal distribution of the C−C distances: the average hexagon−hexagon bond is 1.39(1) Å, while the average hexagon−pentagon bond is 1.45(1) Å. The distances between the centre of the ball and the 30 independent carbon atoms vary from 3.53(1) to 3.56(1) Å. An analysis of the distances between the centre of the ball and the 30 independent carbon atoms does not indicate any systematic deformation, such as is found in the ionic structure of decamethylnickelocenium fulleride.[22]

The crystal structure of **1** is quite different from that of the $C_{60}Fc_2$ adduct,[14] in which only one ring of the single ferrocene molecule faces (with a sideways slipping of 0.8 Å) a fullerene pentagon in an almost eclipsed way.

In order to carry out a more accurate comparison of the *Fc molecules in **1** with the same molecule alone, we also redetermined the crystal structure of *Fc, at 150 K. However, the resulting resolved structure did not substantially differ from that reported by Freyberg et al.,[32] which was carried out at room temperature. The molecule has a C_{2h} crystallographic site symmetry with the iron atom sitting on an inversion centre, and so the two cyclopentadienyl rings must be exactly staggered. The three independent Fe−C, C−C, and $C-CH_3$ distances and the C−C−C angles differ by less than 3σ and their average values are reported in Table 1. With respect to the plane through the five-membered rings, the methyl carbon atoms are slightly (about 0.06 Å) displaced in the direction away from the central Fe atom. In all the methyl groups, two hydrogen atoms point towards the Fe and are relatively close to the cyclopentadienyl plane, while the third H sticks out of the plane away from the Fe. This pattern was also found in a series of $Fe(Me_4RCp)_2$ derivatives.[33,34]

The two different *Fc molecules in compound **1** are somewhat less regular than in *Fc alone; nevertheless, average values of selected distances and angles are very similar in the two structures. Table 1 summarises the most significant distance and angle values for A and B in **1**, in comparison with those in *Fc. The disposition of the methyl groups

Table 1. Main geometrical parameters of the *Fc moiety from the crystal structure of adduct **1**, in comparison with *Fc alone

	Adduct **1** − molecule A			Adduct **1** − molecule B			*Fc
Distance [Å]	Minimum	Maximum	Average	Minimum	Maximum	Average	Average
Fe−C	2.038(6)	2.068(6)	2.053(6)	2.035(7)	2.063(7)	2.047(7)	2.053(2)
C−C	1.417(9)	1.437(9)	1.428(9)	1.397(10)	1.440(10)	1.416(10)	1.430(3)
$C-CH_3$	1.489(9)	1.519(9)	1.508(9)	1.477(10)	1.529(10)	1.509(11)	1.500(3)
Angle [°]							
C−C−C	107.3(6)	109.0(6)	108.0(6)	105.5(7)	109.2(7)	108.0(7)	108.0(2)

is similar to that found in *Fc alone, and their deviations from the cyclopentadienyl plane are also of the same order of magnitude and in the same direction.

Solid-State ^{13}C NMR

The ^{13}C CPMAS spectrum of **1** shows the presence of five resonances, at δ = 142.1, 79.9, 79.3, 78.8, and 10.8 ppm. The low-field resonance falls in the range typical of the C_{60} peak. The fact that all 60 carbon atoms are equivalent indicates that rapid isotropic motion of C_{60} on the NMR timescale is occurring in the solid at room temperature.[35−36] This result is apparently in conflict with the X-ray data, which allow complete refinement of the fullerene structure, but one should consider the different measurement temperatures and the different timescales involved in X-ray and NMR analyses.[37] Unfortunately, further attempts to observe the static ^{13}C CPMAS spectrum at low temperature were precluded by the low signal/noise ratio, probably due to the increasing of relaxation times with decreasing temperature.

The three resonances in the range δ = 70−80 ppm can readily be assigned to the cyclopentadienyl carbon atoms. Bearing in mind that inequivalences in the solid state can arise from the crystal packing, these data are in full agreement with the solid-state structure, which shows the presence of three different environments for the *Cp rings. The single resonance found for each *Cp ligand in the ^{13}C CPMAS spectrum is an indication that the rings are in a fast rearrangement process in the solid state. As previously shown in the case of *Fc,[38] the dynamic process corresponds to a rotation of the *Cp rings in the planes perpendicular to their C_5 coordination axes. Finally, the resonance at higher field appears as a broad signal due to partial overlapping of the slightly different methyl ligands.

Vibrational Spectra

The infrared and Raman features of adduct **1** are nearly coincident with those of the two separated components, as Figures 3 and 4 clearly show. Table 2 reports the frequency values and the assignments. In particular, neither the different crystallographic position of the *Fc molecules, nor the different orientations of the *Cp rings strongly affect the vibrational behaviour.

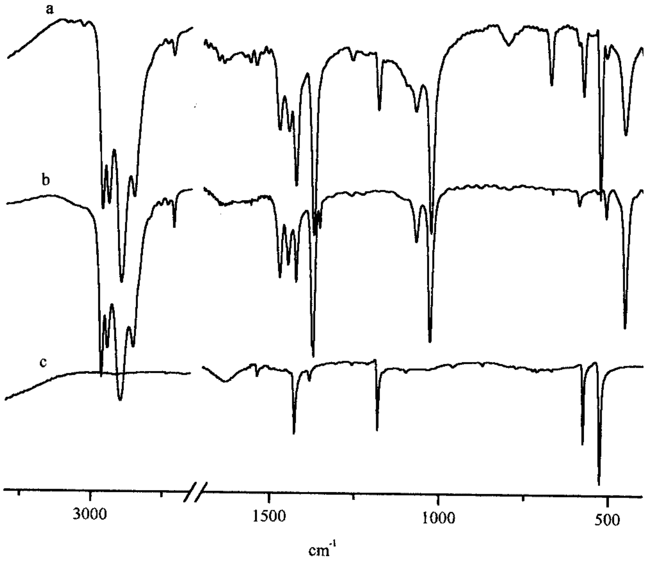

Figure 3. Infrared spectra (KBr disk) of (a) adduct **1**, (b) *Fc, (c) C_{60}

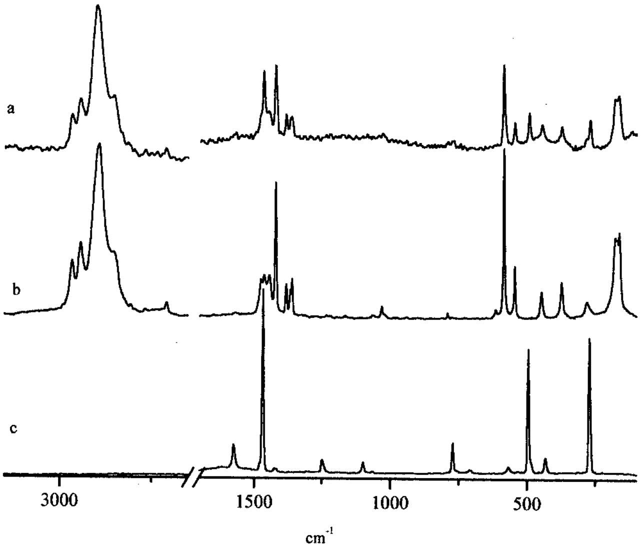

Figure 4. Raman spectra (crystals) of (a) adduct **1**, (b) *Fc, (c) C_{60}

Adduct 2

The adduct **2** was always obtained only in trace amounts, as a faint light brown powder accompanying the crystals of adduct **1**. Any attempt to recrystallise the powder failed: the result was the recovery of the starting components. The only reliable experimental data that we were able to obtain are the infrared and Raman spectra in the solid state. Although the vibrational patterns of *Fc and C_{60} would not be expected to change greatly as a consequence of electron transfer,[39] a careful examination finds significant differences. First of all, the ν(CH) pattern is significantly shifted towards higher frequency by ca. 6−8 cm^{-1} and it is surprisingly similar to that of the adduct [*Fc][TCNE] (TCNE = tetracyanoethylene), for which an ionic structure is proposed.[40] In a recent study on the spectra of permethylated metallocene complexes we proposed the shift of the ν(CH) modes as a measure of the positive charge on the metallocene unit.[31] In order to allow a quantitative estimate of this effect, we compared the frequency of the most intense Raman band in this region, which ranges from 2894 and 2895 cm^{-1} for *Fc and adduct **1** to 2904 cm^{-1} for adduct **2**, to 2919 cm^{-1} for the TCNE adduct, and up to 2926 cm^{-1} for the PF_6^- salt. The same trend is shown by the $\delta(CH_3)$ symmetric mode, the frequency of which (1384 cm^{-1}) is close to those in $[*Fc]^+[TCNE]^-$ (1386 cm^{-1}) and $[*Fc]^+[PF_6]^-$ (av. 1385 cm^{-1}) and significantly different from those of *Fc (av. 1375 cm^{-1}) and adduct **1** (av. 1372 cm^{-1}).

Even more interesting is the Raman pattern between 1600 and 1350 cm^{-1}. This includes some $\delta(CH_3)$ and ν(CC)

Table 2. Infrared and Raman frequencies [cm^{-1}] and assignment of the vibrational modes of adduct **1**

Infrared	Raman	Assignments
2963 m	2967 w	$\nu_{as}(C-H)$
2942 m	2944 m	$\nu_{as}(C-H)$
2895 s, br	2898 s	$\nu_{s}(C-H)$
2852 m	2852 m, sh	$2\delta(CH_3)$
2713 w	2710 vw	$2\delta(CH_3)$
	1573 m	C_{60} (H_g)
1477 w	ca. 1476 w, br.	$\delta_{as}(CH_3)$
	1466 m	C_{60} (A_{1g})
1449 w	ca. 1445 w	$\delta_{as}(CH_3)$
1427 m		C_{60} (T_{1u})
	1423 m	$\delta_{as}(CH_3)/\nu(C=C)$
	1385 m	$\delta_{s}(CH_3)/\nu(C=C)$
ca. 1375 m, sh		$\delta_{s}(CH_3)$
1371 s	ca. 1370 w, sh	$\delta_{s}(CH_3)$
	1364 m	δ_{s} (CH_3)
1182 m		C_{60} (T_{1u})
1072 w		$\nu(C-CH_3)$
1027 s	1032 w	$\rho(CH_3)$
	772 w	C_{60} (T_{1g})
674 w		
	587 s	Cp ring breathing
577 m		C_{60} (T_{1u})
	547 m	asym. tilt(Cp−Fe−Cp)
528 s		C_{60} (T_{1u})
	495 m	C_{60} (A_{1g})
453 m, br	450 w	$\nu_{as}(Cp-Fe)$
	431 w	C_{60} (H_g)
381 vw	375 w	sym. tilt(Cp−Fe−Cp)
	ca. 284 w	
	272 m	C_{60} (H_g)
	179 s	$\nu_{s}(Cp-Fe)$
	165 s	$\nu_{s}(Cp-Fe)$

modes of *Fc and the highest frequency modes − $H_g(8)$, $H_g(7)$, and $A_g(2)$ − of C_{60}. In Figure 5 the Raman spectrum of adduct **2** is compared with those of *Fc and C_{60}: the difference in the frequency and in the shape of the bands is clearly evident. More informative data can be obtained by a deconvolution of the spectral pattern between 1550 and 1350 cm^{-1}. Figure 6 shows the experimentally measured spectrum and the fitted curve obtained as a sum of five mixed Lorentzian/Gaussian curves centred at 1475, 1451, 1423, 1384, and 1367 cm^{-1}. The good quality of the matching between the experimentally measured and the fitted curve is shown by the value of the correlation coefficient (0.99857). The band at 1451 cm^{-1} is attributable to the $A_g(2)$ mode of C_{60} (the others are *Fc modes). The $H_g(8)$ mode appears at 1562 cm^{-1}.[41] These modes show significant low-energy shifts of 12 and 16 cm^{-1} for H_g and A_g, respectively. Other C_{60} modes show similar shifts: such as A_g, from 495 to 486 cm^{-1}, and H_g, from 271 to 249 cm^{-1}. In addition, the bands of adduct **2** are clearly broadened with respect to those of C_{60} [e.g., the full width at half maximum (fwhm) of the $A_g(2)$ mode is ca. 22 cm^{-1} for adduct **2** and ca. 6 cm^{-1} for C_{60} alone]. Both effects have been already reported for the compound C_{60}/TDAE and ascribed to electron-transfer from TDAE to C_{60}.[28] All the vibrational data and assignments are listed in Table 3.

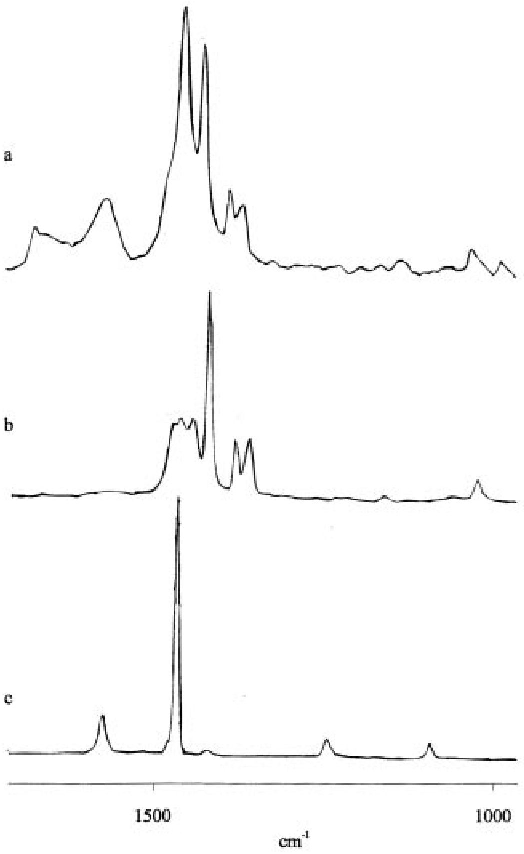

Figure 5. Raman spectra (crystals) in the 1600−1000 cm^{-1} range for (a) adduct **2**, (b) *Fc, (c) C_{60}

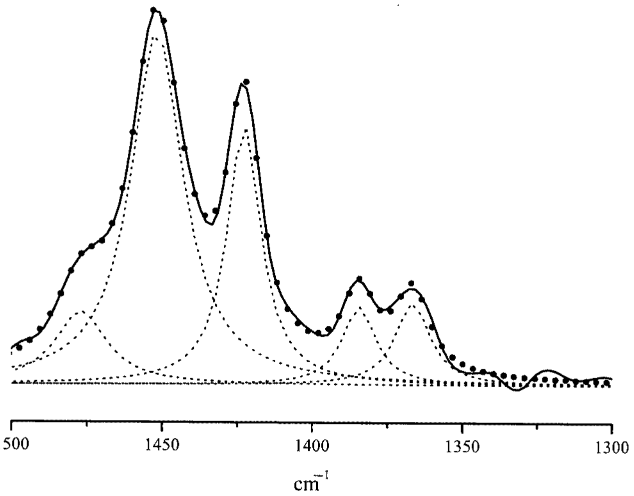

Figure 6. Deconvolution of the Raman band pattern in the 1500−1300 cm^{-1} range for the adduct **2**; the solid line is the experimentally measured spectrum; the small dashed lines are the individual fitted curves and the dots indicate the resultant fitted curve

A Comparison with Fc_2C_{60} Adduct

The molecular structure of this adduct was described almost ten years ago.[14] The crystal packing of the Fc molecules is simpler than that shown in adduct **1**. Only one Fc molecule in a general crystallographic position is present

Table 3. Infrared and Raman frequencies [cm^{-1}] and assignment of the vibrational modes of adduct **2**

Infrared	Raman	Assignments
2960 m	2966 m	$\nu_{as}(C-H)$
	2945 w, sh	$\nu_{as}(C-H)$
2902 m, br.	2904 vs	$\nu_s(C-H)$
2854 w	2851 w, sh	$2\delta(CH_3)$
	1562 m, br.	C_{60} (H_g)
	ca. 1475 m, sh	$\nu(C=C)$
	1451 s	C_{60} (A_{1g})
1428 s		C_{60} (T_{1u})
	1423 m	$\delta_{as}(CH_3)/\nu(C=C)$
1383 s	1384 w	$\delta_{as}(CH_3)/\nu(C=C)$
	1367 w	$\delta_s(CH_3)/\nu(C=C)$
1182 m		C_{60} (T_{1u})
1027 m	1034 w, br.	$\rho(CH_3)$
	991 w	
	858 w, br.	C_{60} (T_{1g})
	708 w	
674 w		
	586 s	Cp ring breathing
576 m		C_{60} (T_{1u})
	546 m	asym. tilt(Cp−Fe−Cp)
526 vs		C_{60} (T_{1u})
	486 m, br.	C_{60} (A_{1g})
454 m, br.	447 w	$\nu_{as}(Cp-Fe)$
	374 m	symm. tilt(Cp−Fe−Cp)
	ca. 282 w, br.	
	229 w	
	177 s, sh	$\nu_s(Cp-Fe)$
	164 s	$\nu_s(Cp-Fe)$

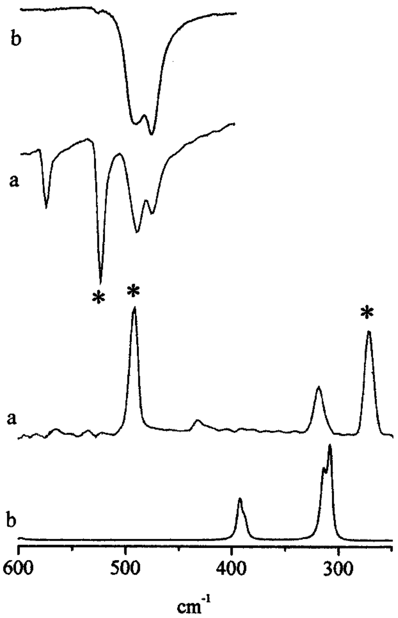

Figure 7. Infrared (top curves, KBr disk) and Raman (bottom curves, crystals) spectra of Fc_2C_{60} adduct (a) and Fc (b); the bands marked with * correspond to C_{60} modes

and only one Cp ring faces one of the C_{60} pentagons. We explored its spectroscopic features further.

The ^{13}C CPMAS spectrum is consistent with the crystal structure. Two peaks of equal intensity at $\delta = 71.09$ and 72.20 ppm are attributable to the cyclopentadienyl carbon atoms. The splitting of the expected unique peak is consistent with the different environments of the two rings, due to the proximity of one ring to the C_{60} cage. A resonance at $\delta = 144.43$ ppm is attributable to the C_{60} carbon atoms. The narrowness of the peak and the absence of spinning side bands confirm the high mobility of the fullerene molecule at room temperature.

At very first sight, the infrared and Raman spectra appear as a simple superpositions of the spectra of the single components, but careful inspection reveals that some spectral features differ significantly, in that the bands show small frequency shifts or changes in their relative intensities. This is particularly evident in the 3200−3000 cm^{-1}, 900−800 cm^{-1}, and 500−300 cm^{-1} regions, which are typical of the ν(CH), γ(CH), and Fe−ring stretching modes. Not surprisingly, they belong to the vibrations that, more than the others, are involved in possible interactions between the Cp rings and fullerene. See, for instance, Figure 7, which shows the spectra of Fc and Fc_2C_{60} in the low-wavenumber region. The intensity and the frequency of the infrared and Raman features corresponding to the skeletal motion of the Fc unit in the Fc_2C_{60} adduct are significantly different from those of Fc alone, presumably reflecting the interaction of one Cp ring with C_{60}. On the other hand, the bands of the C_{60} component also show small but significant changes with respect to those of the free C_{60}. Thus, the Raman feature at 493 cm^{-1}, the totally symmetric A_g breathing mode of the cage,[42,43] which can be expected to interact with the sym. Cp−Fe−Cp stretching, is clearly shifted (2.5 cm^{-1}). In addition, the band at 1464 cm^{-1}, regarded as a measure of electron transfer from the donor metallocene to C_{60}, shows a small (4 cm^{-1}) low-energy shift. Other figures (Figures S1 and S2), illustrating selected regions of the spectra, and a table (Table S1), listing the frequency data and assignment, are included as Supporting Information (see also footnote on the first page of this article).

Conclusion

The formation of co-crystals of organic and organometallic species with fullerene molecules is governed both by structural and by electronic aspects: a curved surface of co-blocks[44] allows a better fit in the formation of a solid-state complex structure, and the interaction of the electron acceptor C_{60} with good electron-donating systems is thermodynamically favoured. Nevertheless, the fullerene species exhibit behaviour determined by the aromatic character of its bonds and, like planar aromatic molecules, are able to enter into intermolecular interactions through the π electron density, without net electron transfer between the C_{60} and a donor molecule. For example, the C_{60} benzene solvate[45] can be viewed as a co-crystal between C_{60} and C_6H_6. The benzene rings are parallel to the surface of the C_{60} and lie over the (6,6) bond, where the electron density is most localized. Similarly, the facing of the pentagonal ring of C_{60} with the five-carbon ring of the permethylated ferrocene may suggest an interaction between the HOMO of the *Fc and the LUMO of C_{60}.

While **1** is undoubtedly a molecular adduct, the vibrational data suggest that the minor product **2** has an ionic structure, similar to those of $Cp*_2Mn/C_{60}$, $Cp*_2Ni/C_{60}$, and bis(toluene)$_2$Cr/C_{60}.[46] In the absence of any other experimental support, we are confident that the vibrational behaviour is a strong indicator of the charge transfer between the donor and the acceptor molecules, as it has been demonstrated for C_{60}[28] and *Fc[31], separately linked to other species. In this light, the spectra also suggest a small degree of electron transfer from Fc to C_{60} in the Fc_2C_{60} molecular adduct.

Experimental Section

Reactants and Solvents: All manipulations were performed by standard Schlenk techniques under an inert gas. C_{60} was purchased from Hoechst and used without further purification. *Fc (Aldrich) was purified by sublimation. The solvents were distilled from sodium (benzene and toluene) or P_4O_{10} (1,2-dichlorobenzene) and then stored under argon.

Synthesis of Adducts of *Fc and C_{60}: The preparation of intermolecular adducts of C_{60} is influenced by the starting material's low solubility. Solvents able to dissolve both *Fc and C_{60} significantly are benzene, toluene, and 1,2-dichlorobenzene. Any attempted cocrystallisation in these solvents by changing the stoichiometric ratio between *Fc and C_{60} always gave the same results: well-shaped, black crystals of adduct **1**, mixed with a small amount of light brown powder identified as the adduct **2**. In a typical preparation, C_{60} (50 mg, 0.069 mmol) was dissolved in benzene (35 mL) in a Schlenk tube and mixed with *Fc (45 mg, 0.14 mmol), previously dissolved in a few drops of benzene. The solution was slowly concentrated under an inert gas in a dry-box. After concentration, a thin layer of light brown dust mixed with black, lustrous crystals had deposited on the wall of the tube. The excess of deposited *Fc was removed by sublimation. The two compounds were mechanically separated from the solid mixture. Shiny black crystals of adduct **1** suitable for X-ray analysis were obtained by recrystallization of a 1,2-dichlorobenzene solution of the crude product at −30 °C.

X-ray Crystal Structure Analyses: Crystallographic data and details of data collection and refinement for adduct **1** and *Fc[47] are given in Table 4. Both sets of data collection were carried out with a four-circle automatic diffractometer at 150 K. Structure solutions were obtained by direct methods and refinements by full-matrix, least squares on F^2 (non-H atoms with anisotropic displacement parameters, H atoms geometrically positioned and treated as riding atoms). The computer programs used were: XSCANS[48] for data collection, SIR92[49] for structure solution, SHELXL-97[50] for structure refinement and MOLDRAW[51] and XP[52] for graphic analysis.

NMR Spectra: The ^{13}C CPMAS spectrum was acquired with a Jeol GSE-270 spectrometer operating at 67.8 MHz. The MAS rotor was spun with air at ca. 5.2 kHz, the contact time was 3.5 ms and the recycle delay 10 s. The Hartmann−Hann condition was optimised with hexamethylbenzene. ^{13}C chemical shifts are given in ppm from external tetramethylsilane reference.

Infrared Spectra: The infrared spectra were collected with a Bruker Equinox 55 FT-IR spectrophotometer, with a resolution of 2 cm^{-1} and an average 64 scans.

Table 4. Crystal data and structure refinement parameters for adduct **1** and *Fc

Compound	Adduct **1**	*Fc
Empirical formula	$(C_{120}H_{90}Fe_3)/2$	$C_{20}H_{30}Fe$
Formula mass	849.74	326.29
Crystal system	monoclinic	orthorhombic
Space group	$P2_1/c$	*Cmca*
a [Å]	10.287(11)	15.113(4)
b [Å]	20.199(14)	11.592(3)
c [Å]	19.932(17)	9.958(3)
β [°]	100.29(4)	90
V [Å^3]	4075(6)	1744.5(8)
Z	4	4
F(000)	1776	704
Density (calcd.) [g cm^{-3}]	1.385	1.242
Temperature [K]	150(2)	
Diffractometer	Siemens P4	
Radiation (graph-monochr.) [Å]	0.71073	
Absorption coefficient [mm^{-1}]	0.584	0.857
Crystal size [mm]	0.20×0.23×0.48	0.22×0.44×0.46
Colour	black	orange
Shape	prism	prism
Scan method	ω	
Scan speed [°/min]	variable: 3.0−20.0	
Scan range [°]	0.90	1.40
θ range [°]	1.5−25.0	1.5−35.0
Index ranges	$-6 \le h \le 12$, $-6 \le k \le 24$, $-4 \le l \le 23$	$0 \le h \le 24$, $0 \le k \le 18$, $-16 \le l \le 0$
Reflections collected	5869	1995
Independent reflections	5750	1981
Absorption correction	n/a	n/a
Refinement method	Full-matrix, least-squares on $\lvert F_o\rvert^2$	
Observed reflections	3086 $[I > 2\sigma(I)]$	1354 $[I > 2\sigma(I)]$
Data/restraints/parameters	5750/0/556	1981/0/62
Goodness of fit on $\lvert F_o\rvert^2$	1.088	1.040
R indices $[I > 2\sigma(I)]$	$R1 = 0.0621$, $wR2 = 0.1194$	$R1 = 0.0470$, $wR2 = 0.1006$
R indices (all data)	$R1 = 0.1543$, $wR2 = 0.1647$	$R1 = 0.0841$, $wR2 = 0.1159$
Largest diff. peak and hole [e·Å^{-3}]	0.439, −0.436	0.590, −0.715
Weight (calculated)	$w = 1/[\sigma^2(\lvert F_0\rvert^2) + (gP)^2 + qP]$, $P = (\lvert F_0\rvert^2 + 2\lvert F_c\rvert^2)/3$	
	$g = 0.054$, $q = 3.352$	$g = 0.049$, $q = 1.030$

Raman Spectra: The Raman spectra were collected with a Bruker RFS 100 FT Raman spectrophotometer, by use of NIR laser radiation at 1064 nm and a Ge diode (laser power 100 mW, res. 4 cm^{-1}). To minimize decomposition of the sample, the complexes were sealed in capillary glass tubes under nitrogen. Adduct **2**, which shows a significant fluorescence background, required low laser power (30 mW) and an average of 2000 scans, obtained by a sequence of several scan-packets (50−100 scans each) to give a good spectrum.

Acknowledgments

Financial support from the MIUR (COFIN 2000 to E. D., R. G. and P. L. S.) is gratefully acknowledged.

[1] P. W. Stephens, D. Cox, J. W. Lauher, L. Mihaly, J. B. Wiley, P. M. Allemand, A. Hirsch, K. Holczer, Q. Li, J. D. Thompson, F. Wudl, *Nature* **1992**, *355*, 331.

[2] W. J. Blau, J. H. Byrne, D. J. Cardin, T. J. Dennis, J. P. Hare, H. W. Kroto, R. Taylor, D. R. M. Walton, *Phys. Rev. Lett.* **1991**, *67*, 1423.

[3] R. Taylor, D. R. M. Walton, *Nature* **1993**, *363*, 685.

[4] D. M. Guldi, *Chem. Commun.* **2000**, 321.

[5] Q. Xie, E. Pérez-Cordero, L. Echegoyen, *J. Am. Chem. Soc.* **1992**, *114*, 3978.

[6] Y. Ohsawa, T. Saji, *J. Chem. Soc., Chem. Commun.* **1992**, 781.

[7] I. Noviandri, R. D. Bolskar, P. A. Lay, C. A. Reed, *J. Phys. Chem. B* **1997**, *101*, 6350.

[8] L. Echegoyen, L. E. Echegoyen, *Acc. Chem. Res.* **1998**, *31*, 593.

[9] C. A. Reed, R. D. Bolskar, *Chem. Rev.* **2000**, *100*, 1075.

[10] A. F. Hebard, M. J. Rosseinsky, R. C. Haddon, D. W. Murphy, S. H. Glarum, T. T. M. Palstra, A. P. Ramirez, A. R. Kortan, *Nature* **1991**, *350*, 600.

[11] D. W. Murphy, M. J. Rosseinsky, R. M. Fleming, R. Tycko, A. P. Ramirez, R. C. Haddon, T. Siegrist, G. Dabbagh, J. C. Tully, R. E. Walstedt,, *J. Phis. Chem. Solids* **1992**, *53*, 1321.

[12] *Anthracene:* J. A. Schlueter, J. M. Seaman, S. Taha, H. Cohen, K. R. Lykke, H. H. Wang, J. M. Williams, *J. Chem. Soc., Chem. Commun.* **1993**, 972.

[13] $Fe_4(CO)_4(\eta^5\text{-}C_5H_5)_4$: J. D. Crane, P. B. Hitchcock, *J. Chem. Soc., Dalton Trans.* **1993**, 2537.

[14] *Ferrocene:* J. D. Crane, P. B. Hitchcock, H. W. Kroto, R. Taylor, D. R. M. Walton, *J. Chem. Soc., Chem. Commun.* **1992**, 1764.

[15] *N,N-Diethylaniline:* Y. Wang, *J. Phys. Chem.* **1992**, *96*, 764.

[16] *1,4-Diazabicyclooctane:* K. I. Priyadarsini, H. Mohan, A. K. Tyagi, J. P. Mittal, *Chem. Phys. Lett.* **1994**, *230*, 317.

[17] *Hexamethylenetetratellurafulvalene:* T. Pradeep, K. K. Singh, A. P. B. Sinha, D. E. Morris, *J. Chem. Soc., Chem. Commun.* **1992**, 1747.

[18] *Bis(ethylenedithio)tetrathiafulvalene:* A. Izuoka, T. Tachikawa, T. Sugawara, Y. Suzuki, M. Konno, Y. Saito, H. Shinohara, *Chem. Commun.* **1992**, 1472.

[19] *Triethylamine:* Y. A. Sun, B. Ma, G. E. Lawson, *Chem. Phys. Lett.* **1995**, *233*, 57.

[20] P_4: R. E. Douthwaite, M. L. H. Green, S. J. Heyes, M. J. Rosseinsky, J. F. C. Turner, *J. Chem. Soc., Chem. Commun.* **1994**, 1367.

[21] *Hydroquinone:* O. Ermer, *Helv. Chim. Acta* **1991**, *74*, 1339.

[22] $\text{-}C_5(CH_3)_5]_2Ni$: W. C. Wan, (X^5. Liu, G. M. Sweeney, W. E. Broderick, *J. Am. Chem. Soc.* **1995**, *117*, 9580.

[23] G. A. Heath, J. E. Mc Grady, R. L. Martin, *J. Chem. Soc., Chem. Commun.* **1992**, 1272.

[24] J. Stinchcombe, A. Pénicaud, P. Bhyrappa, P. W. D. Boyd, C. A. Reed, *J. Am. Chem. Soc.* **1993**, *115*, 5212.

[25] M. L. Mc Glashen, M. E. Blackwood Jr., T. G. Spiro, *J. Am. Chem. Soc.* **1993**, *115*, 2074.

[26] Y. Zhang, Y. Du, J. R. Shapeley, M. J. Weaver, *Chem. Phys. Lett.* **1993**, *205*, 6; Y. Zhang, Y. Du, J. R. Shapeley, M. J. Weaver, *Chem. Phys. Lett.* **1993**, *205*, 6, 508.

[27] J. Fulana, M. Jakobi, J. P. Maier, *Chem. Phys. Lett.* **1993**, *21*, 43; J. Fulana, M. Jakobi, J. P. Maier, *Chem. Phys. Lett.* **1993**, *21*, 43, 227.

[28] D. V. S. Muthu, M. N. Shashikala, A. K. Sood, R. Seshadri, C. N. R. Rao, *Chem. Phys. Lett.* **1994**, *217*, 146.

[29] K. Tanaka, T. Sato, T. Yamabe, *J. Phys. Chem.* **1996**, *100*, 3980.

[30] E. Diana, R. Rossetti, P. L. Stanghellini, S. F. A. Kettle, *Inorg. Chem.* **1997**, *36*, 382.

[31] P. L. Stanghellini, E. Diana, E. Boccaleri, R. Rossetti, *J. Organomet. Chem.* **2000**, *593−594*, 36.

[32] D. P. Freyberg, J. L. Robbins, K. N. Raymond, J. C. Smart, *J. Am. Chem. Soc.* **1979**, *101*, 892.

[33] U. Siemeling, U. Vorfeld, B. Neumann, H. G. Stammler, *Chem. Ber.* **1995**, *128*, 481.

[34] M. Hobi, O. Ruppert, V. Gramlich, A. Togni, *Organometallics* **1997**, *16*, 1384.

[35] C. S. Yannony, R. D. Jonson, G. Meijer, D. S. Bethune, J. R. Salem, *J. Phys. Chem.* **1991**, *95*, 9.

[36] H. He, J. Barras, J. Foulkes, J. Klinowski, *J. Phys. Chem. B* **1996**, *101*, 117.

[37] P. Day, in: *The Time Domain in Surface and Structural Dynamics* (Eds.: G. J. Long, F. Grandjean), Kluwer Academic Publishers, The Netherlands, **1987**, p. 1.

[38] D. E. Wemmer, D. J. Ruben, A. Pines, *J. Am. Chem. Soc.* **1981**, *103*, 28.

[39] T. Pradeep, K. K. Swigh, A. P. B. Sinha, D. E. Harris, *J. Chem. Soc., Chem. Commun.* **1992**, 1747.

[40] E. Adman, M. Rosenblum, S. Sullivan, T. N. Margulis, *J. Am. Chem. Soc.* **1967**, *89*, 4540.

[41] The remaining mode, $H_g(7)$, gives rise to a weak band at 1423 cm^{-1} in the Raman spectrum of C_{60} and cannot be detected by the deconvolution procedure.

[42] R. E. Stanton, M. D. Newton, *J. Phys. Chem.* **1988**, *92*, 2141.

[43] C. H. Choi, M. Kertesz, L. Mihaly, *J. Phys. Chem. A* **2000**, *104*, 102.

[44] T. Ishii, N. Aizawa, M. Yamashita, H. Matsuzaka, T. Kodama, K. Kikuchi, I. Ikemoto, Y. Iwasa, *J. Chem. Soc., Dalton Trans.* **2000**, 4407.

[45] M. F. Meidine, P. B. Hitchcock, H. W. Kroto, R. Taylor, D. R. M. Walton, *J. Chem. Soc., Chem. Commun.* **1992**, 1534.

[46] A. Hönnerscheid, L. van Wüllen, M. Jansen, *J. Chem. Phys.* **2001**, *115*, 7161.

[47] Supplementary material (coordinates of H atoms, anisotropic thermal parameters, bond lengths and angles) has been deposited at the Cambridge Crystallographic Data Centre, with deposition numbers CCDC-190842 (**1**) and -190841 (*Fc) at 150 K.

[48] Bruker, *P3/PC Diffractometer Program*, Version 3.13, Bruker Analytical X-ray Systems, Inc., Madison, Wisconsin, USA, **1989**.

[49] A. Altomare, G. Cascarano, C. Giacovazzo, A. Guagliardi, M. C. Burla, G. Polidori, M. Camalli, *J. Appl. Crystallogr.* **1994**, *27*, 435.

[50] G. M. Sheldrick, *SHELXL-97*, University of Göttingen, Germany, **1997** (website: http://shelx.uni-ac.gwdg.de/SHELX/).

[51] P. Ugliengo, D. Viterbo, G. Chiari, *Z. Kristallogr.* **1993**, *207*, 9 (website: http://www.ch.unito.it/ifm/fisica/moldraw/moldraw.html).

[52] G. M. Sheldrick, *SHELXTL/IRIS*, Bruker Analytical X-ray Systems, Inc., Madison, Wisconsin, USA, **1990**.

Received August 7, 2002
[I02447]